Naval Research Laboratory

Washington, DC 20375-5320

NRL/MR/6812--20-10,136

Germanium-Tin Materials Development for Optoelectronics

Dr. Glenn Jernigan
Dr. Nadeem Mahadik
Dr. Mark Twigg
Dr. Jill Nolde
Dr. Chaffra Affouda
Dr. Eric Jackson

Optoelectronics and Radiation Effects Branch
Electronics Science and Technology Division

August 17, 2020

DISTRIBUTION STATEMENT A: Approved for public release, distribution is unlimited.

UNCLASSIFIED//DISTRIBUTION A

REPORT DOCUMENTATION PAGE

Form Approved OMB No. 0704-0188

Public reporting burden for this collection of information is estimated to average 1 hour per response, including the time for reviewing instructions, searching existing data sources, gathering and maintaining the data needed, and completing and reviewing this collection of information. Send comments regarding this burden estimate or any other aspect of this collection of information, including suggestions for reducing this burden to Department of Defense, Washington Headquarters Services, Directorate for Information Operations and Reports (0704-0188), 1215 Jefferson Davis Highway, Suite 1204, Arlington, VA 22202-4302. Respondents should be aware that notwithstanding any other provision of law, no person shall be subject to any penalty for failing to comply with a collection of information if it does not display a currently valid OMB control number. **PLEASE DO NOT RETURN YOUR FORM TO THE ABOVE ADDRESS.**

1. REPORT DATE *(DD-MM-YYYY)*
17-08-2020

2. REPORT TYPE
NRL Memorandum Report

3. DATES COVERED *(From - To)*
FY17 – FY20

4. TITLE AND SUBTITLE
Germanium-Tin Materials Development for Optoelectronics

5a. CONTRACT NUMBER

5b. GRANT NUMBER

5c. PROGRAM ELEMENT NUMBER
61153N

6. AUTHOR(S)
Dr. Glenn Jernigan, Dr. Nadeem Mahadik, Dr. Mark Twigg, Dr. Jill Nolde,
Dr. Chaffra Affouda, and Dr. Eric Jackson

5d. PROJECT NUMBER

5e. TASK NUMBER

5f. WORK UNIT NUMBER
1G51

7. PERFORMING ORGANIZATION NAME(S) AND ADDRESS(ES)
Naval Research Laboratory
4555 Overlook Avenue, SW
Washington, DC 20375-5320

8. PERFORMING ORGANIZATION REPORT NUMBER
NRL/MR/6812--20-10,136

9. SPONSORING / MONITORING AGENCY NAME(S) AND ADDRESS(ES)
Naval Research Laboratory
4555 Overlook Avenue, SW
Washington, DC 20375-5320

10. SPONSOR / MONITOR'S ACRONYM(S)

11. SPONSOR / MONITOR'S REPORT NUMBER(S)

12. DISTRIBUTION / AVAILABILITY STATEMENT

DISTRIBUTION STATEMENT A: Approved for public release; distribution is unlimited.

13. SUPPLEMENTARY NOTES

14. ABSTRACT

A new approach to communications, shortwave (SWIR), and midwave infrared (MWIR) optoelectronics, based on the growth of direct gap Ge-Sn alloys on silicon, via an intermediate SiGeSn virtual substrate (VS) is presented. Direct growth of optoelectronics on Si will allow easy, robust integration of lasers and detectors on Si readout integrated circuits (ROICs). We successfully developed SiGeSn alloys that are single-crystalline, optically-thick (up to 500 nm), and fully-relaxed with a large lattice constant (up to 5.75 Å) for use as a VS grown on a Si (100) surface. We demonstrate the growth of an 800 nm Ge0.88Sn0.12 alloy formed on the SiGeSn VS that has a direct bandgap absorption at 3.3 µm in the MWIR.

15. SUBJECT TERMS
Optoelectronics Germanium Tin Silicon Ge Sn GeSn Infrared Detectors
Shortwave Midwave SWIR MWIR Molecular Beam Epitaxy MBE

16. SECURITY CLASSIFICATION OF:			17. LIMITATION OF ABSTRACT	18. NUMBER OF PAGES	19a. NAME OF RESPONSIBLE PERSON
a. REPORT	b. ABSTRACT	c. THIS PAGE			Glenn G. Jernigan, Ph.D.
Unclassified Unlimited	Unclassified Unlimited	Unclassified Unlimited	Unclassified Unlimited	20	19b. TELEPHONE NUMBER *(include area code)* (202) 404-8544

Standard Form 298 (Rev. 8-98)
Prescribed by ANSI Std. Z39.18

UNCLASSIFIED//DISTRIBUTION A

This page intentionally left blank.

CONTENTS

1. INTRODUCTION 1
  1.1 Objective 1
  1.2 Motivation 1
2. APPROACH 3
  2.1 Molecular Beam Epitaxy (MBE) versus Chemical Vapor Deposition 3
  2.2 Ge, GeSn, and SiGeSn Virtual Substrates on Si 4
3. EXPERIMENTS 5
  3.1 Sn and GeSn on Ge VS 5
    3.1.1 Sn on Ge and Ge on Sn Studies 6
    3.1.2 GeSn on Ge VS 7
    3.1.3 Sb Surfactant Assisted GeSn Growth on Ge VS 9
  3.2 Sn Reactivity on Various Surfaces 10
    3.2.1 Sn on Si, Ge, and Sapphire 10
    3.2.2 Co-depositing Sn and Si on Sapphire 10
  3.3 Developing a SiGeSn VS 11
    3.3.1 SiGeSn on Ge (100) and Ge VS 11
    3.3.2 SiGeSn on Si (100) 12
  3.4 GeSn on SiGeSn 14
4. CONCLUSIONS 14

This page intentionally left blank.

EXECUTIVE SUMMARY

We present a new, and potentially revolutionary, approach to communications, shortwave (SWIR), and midwave infrared (MWIR) optoelectronics, based on the growth of direct gap Ge-Sn alloys on silicon, via an intermediate SiGeSn virtual substrate (VS). Direct growth of optoelectronics on Si will allow easy, robust integration of lasers and detectors on computer processors and avoid the current pixel size limitations for IR detectors due to the requirements of indium bumps when hybridizing III-V pixels to Si readout integrated circuits (ROICs). Although Sn has very low solubility in Ge (less than 2%), we report the successful incorporation of 13% Sn in Ge using kinetically-limited, low-temperature molecular beam epitaxy. Initial studies showed that Sn adatoms have a high surface mobility, sufficient to overcome the beneficially lower surface free energy of Ge. The use of Sb as a surfactant did increase Sn incorporation, up to 6% in Ge film, but growth of thick films led to loss of crystalline structure. Compressive strain and low Sn reactivity in Ge films was countered by the inclusion of Si atoms in the depositing flux. We successfully developed SiGeSn alloys that are single-crystalline, optically-thick (up to 500 nm), and fully-relaxed with a large lattice constant (up to 5.75 Å) as a VS grown on a Ge (100) surface, on a Ge VS, and on a Si (100) surface. We demonstrate direct bandgap absorption at 3.3 µm in the MWIR from an 800 nm $Ge_{0.88}Sn_{0.12}$ alloy, formed on a SiGeSn VS. Materials improvement in the GeSn and the SiGeSn VS layers are possible and necessary to produce viable IR detectors.

This report presents research conducted by Dr. Glenn Jernigan (6812), Dr. Nadeem Mahadik (6812), Dr. Mark Twigg (6818), Dr. Jill Nolde (6812), Dr. Chaffra Affouda (6812), and Dr. Eric Jackson (6812).

This page intentionally left blank.

Germanium-Tin Materials Development for Optoelectronics

1. INTRODUCTION

1.1 Objective

The successful demonstration of direct bandgap GeSn alloys grown directly on Si substrates via an intermediate virtual substrate (VS) for group-IV optoelectronics in the communications, shortwave, and midwave infrared bands that can be fully integrated with Si technology.

1.2 Motivation

Silicon is an indirect band gap material, and as such, it has poor optoelectronic characteristics (e.g. no stimulated light emission and weak optical absorption near the band gap energy). Conversely, many III-V alloys, having direct band gaps and strong optical coupling, are used in an enormous range of optoelectronic applications. High performance optoelectronic devices, however, require both the strong optical coupling of a direct band-gap semiconductor, and the advanced analog and digital electronic capabilities of silicon. The integration of these two systems has been a difficult challenge and growing optoelectronic III-V materials directly on silicon has been frustrated by three key issues:

1. The lattice constants and coefficients of thermal expansion of most III-V's are much larger than that of silicon, resulting in high compressive strain and high densities of threading dislocations.
2. Silicon and III-V materials are dopants or form deep levels within one another, making intermixing during growth intolerable.
3. III-V bonding is ionic and incompatible with the covalent silicon system, leading to polarized domains and anti-phase boundaries that are strongly detrimental to optoelectronic performance.

For those reasons, III-Vs may never be successfully grown on Si. As a result, the field has largely turned to hybridization techniques such as wafer bonding, transfer printing, and indium bump bonding. For the operation of shortwave (SWIR) and midwave infrared (MWIR) detectors, one of the most critical imaging parameters is the minimum pixel size. Reduction in pixel size is dictated by the practicalities of hybridization with indium bumps (~7 μm) rather than performance needs (< 3 μm). The urgency of this problem is highlighted by the rapid rise of novel heterogeneous integration techniques, but it is not clear that such techniques provide a viable path to diffraction limited optoelectronic device size. Hence, enabling growth of an optoelectronic material that is not a III-V on Si would be highly attractive. Here, we present a new, and potentially revolutionary, approach to communications, SWIR, and MWIR optoelectronics, based on the growth of direct gap Ge-Sn alloys on silicon, via an intermediate SiGeSn virtual substrate (VS), taking advantage of recent developments in the understanding of this alloy system.

Over the past 15 years, Ge has been successfully integrated into the Si electronics industry. Today, we have SiGe alloys (~40% Ge) grown on Si substrates for heterojunction bipolar transistors (HBTs) and complementary metal-oxide-semiconductor transistors (CMOS) devices utilized in radio-frequency (RF) transceivers for cell phone communications (500 MHz–5 GHz). Ge has also been used as implanted material into Si under the source and drain contacts of p-MOSFETs (p-type MOS field effect transistors)

Manuscript approved August 17, 2020.

to compressively strain the Si channel. A compressively strained Si channel has enhanced hole mobility over an unstrained channel. (Nitrogen is implanted under the source/drain in order to place the Si channel in a state of tension within an n-MOSFET and thereby enhance electron mobility.) Although Ge is also an indirect band gap material, there is only a 160 meV difference between the Γ-point (direct gap) and the L-point (indirect gap). It has been known that Ge could become a direct gap material if sufficient tensile strain is applied (in essence to pull the atoms further apart.) In order to place the Ge layer in this degree of tension, it would need to be grown on a substrate with a sufficiently larger lattice parameter to achieve 4.5% uniaxial or 2.5% biaxial tensile strain. A second method for producing a direct band gap in Ge was proposed by Richard Soref in 1993 by forming an alloy with 13% α-Sn [1]. Sn has two allotropes; α-Sn, which is a zero gap semiconductor with a diamond lattice, and β-Sn, which is a distorted tetragonal metal. More recent band structural models predict that the band gap could be direct for alloys with as little as 8% Sn in Ge [2].

Although it has been predicted that a direct band gap is achievable in GeSn alloys, there has been little experimental work that addresses this possibility. A review of the literature (Web of Science) produced a list of less than 700 papers that have been published on GeSn to date. Possibly, the first attempt to grow GeSn was by Greene in 1998, who utilized low-temperature molecular beam epitaxy (LT-MBE) to produce GeSn films with up to 22% Sn [3]. Unlike SiGe, where Si and Ge are completely miscible in each other, Sn has less than 2% solubility in Ge. Hence, any attempt to grow GeSn must necessarily fall within a non-equilibrium regime (kinetically limited and at low temperature). The growth of GeSn on Si generally resulted in large and compressive strains that lead to poor quality films (i.e. high dislocation density) in which a direct band gap was not achieved. In 2005, however, a breakthrough in the growth of a Ge VS on Si was achieved [4], thus making the direct integration of pure (100%) Ge devices on Si possible. The production of a Ge VS also facilitated the growth of GeSn alloys by reducing the potential stress of deposited films. Since the development of the Ge VS, there have been reports of tunable photoluminescence from GeSn alloys (<8% Sn) [5] and of growths of GeSn *p-i-n* diode structures where photodetection and electroluminescence have been observed (<7% Sn) [6]–[11]. We extend the concept of a Ge VS by forming a SiGeSn VS for the growth of an optically active GeSn layer.

2. APPROACH

2.1 Molecular Beam Epitaxy (MBE) versus Chemical Vapor Deposition

Chemical vapor deposition (and metal-organic MO-CVD) are the commercially utilized method for material depositions, as the gas precursors can be made very pure, with a continuous flow system that can control the deposition between 1 nm/s and 100 μm/h. There are, however, a few limitations to the use of CVD. One limitation is the background pressure of gas throughout the growth process, resulting in broadened doping or heterostructure interfaces. The other limitation, which is a significant problem in the growth of SiGeSn, is the high temperature needed to dissociate the precursor molecules on the substrate surface to initiate and propagate growth. The decomposition rate for hydrogen based precursors, silane (SiH_4)[12], germane (GeH_4)[13], and stannane (SnH_4)[14] in homoepitaxy are plotted in Figure 1. This plot shows, that for any growth temperature, the deposition rate for Si, Ge, and Sn is orders of magnitude different. The minimum temperature to dissociate GeH_4 molecule is ~125 °C, but at that temperature, the SnH_4 molecule will dissociate nearly 1000x faster. Therefore, to grow a GeSn alloy, the composition of the gas mixture must account for the desired alloy composition, the different decomposition rates, and the desired total film growth rate to very tight tolerances. For a reasonable CVD growth rate of 1 nm/s, a temperature of 300 °C is needed to dissociate Ge, and at that temperature, the partial pressure of Sn needed is very low, making control of the alloy composition difficult. Much of the GeH_4 precursor is wasted in the CVD growth. The CVD growth process becomes even more complicated and troublesome to grow the SiGeSn tertiary, because the SiH_4 molecule doesn't appreciably decompose until the temperature is > 400 °C. At 400 °C, Sn will segregate and diffuse out of the growing film due to the film strain and its low solubility in Ge and Si. Limited thickness SiGeSn films have been grown [15], where special conditions (temperature, gas pressure, and growth rate) were used before the growth stopped due to the inability to decompose SiH_4. Due to the challenges in CVD growth of SiGeSn, new gaseous precursors are constantly being sought to improve the temperature window for molecular decomposition on a surface and film growth. The Kouvetakis group at Arizona State University has developed a deuteriated Sn species, SnD_4, which is stable for GeSn CVD growth [16], [17], but the cost and complications in producing SnD_4 may make it commercially unviable. Sn-organic precursors (e.g. $Sn(CH_3)_4$, $Sn(CH{=}CH_2)_4$) are both stable and available for CVD growth, but are not desirable as they are extremely toxic.

MBE has been successfully demonstrated to produce GeSn alloys [9], [18], [19] and will be used in this program as well. MBE, as a growth technique, is performed in ultra-high vacuum (< 10^{-9} Torr) to minimize unwanted contaminants and utilizes atomic fluxes of depositing species to grow films with atomic-level control over several microns in thickness. In our case, the atomic fluxes are produced in water cooled, liquid nitrogen shrouded, electron beam heated crucibles. E-beam crucibles are preferred over thermally heated crucibles (Knudsen cells, K-cells) because the deposition rates can be rapidly changed during growth due to the lack of thermal mass/inertia. MBE growth can be performed at any temperature, and for GeSn and SiGeSn alloys, it will be done in a 50–300 °C temperature range. The MBE system also contains *n*-type (P and Sb) and *p*-type (B) dopant K-cells, which will be used to dope the GeSn films. Very few research groups are capable of growing GeSn alloys, and an even smaller number are capable of doing LT-MBE, which is the only technique to have shown the capability of growing GeSn with more than a few percent Sn.

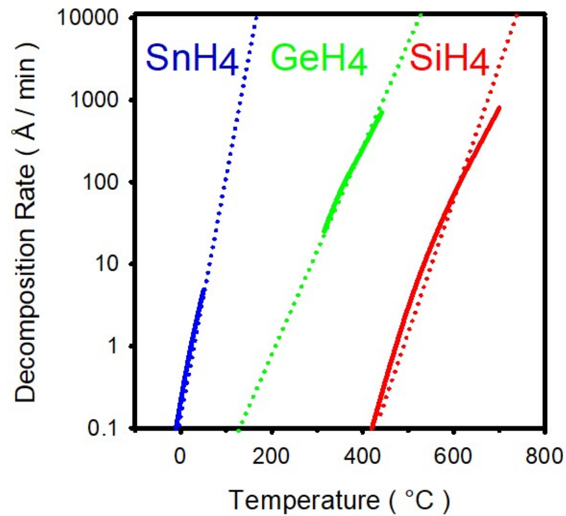

Figure 1. Measured (solid lines) and extrapolated (dotted lines) decomposition rate for the hydrogen-based molecular precursors of Sn, Ge, and Si during homoepitaxial growth by chemical vapor deposition.

2.2 Ge, GeSn, and SiGeSn Virtual Substrates on Si

Heterogeneous integration of Ge optical detectors on Si for high power density applications has been pursued for the realization of high-speed response of the photodiodes under bias [20]. The primary success of those efforts have been the development of a Ge VS on Si. The device development has been hampered by issues with dark current, where a recent report indicated that any Ge material growth will suffer from self-vacancies and self-interstitials [21], [22] when deposited at low temperatures requiring post-growth annealing. A cyclic "step-down" annealing of Ge films (800 °C flash followed by a brief anneal at 700 °C, repeated many times) can reduce Ge dark currents (< 50 μA/cm^2 at −1V bias) in photodiodes by relaxing the film and improving the crystal structure [23]. These high temperature anneals are key to the formation of the Ge VS upon which GeSn can be deposited. The use of a Ge VS has allowed GeSn alloys to be grown beyond the 2% solubility limit with up to 14% Sn [24]. However, due to the compressive stress of GeSn on Ge, these films are not direct band gap and are only grown to a thickness of 50 nm before coherent epitaxy is lost. A new approach has been to grow two layers of GeSn, where the first layer is a GeSn VS allowing for a larger lattice parameter and less compressive stress (i.e. a $Ge_{0.9}Sn_{0.1}$). A recent calculation by Suyog Gupta [25] for the band structure of GeSn alloys grown on a GeSn substrate indicated that all GeSn compositions (0–20% Sn) grown on a VS greater than 8% Sn would result in a direct band gap, as shown in Figure 2 below. Not only would a GeSn VS create a direct band gap, it would also allow for the thicker GeSn films to be grown that are necessary for optical absorption in the vertical (non-waveguide) geometry needed in focal plane arrays. The GeSn VS would also establish the capability for performing band gap engineering by varying Sn and Si composition in Ge, and thereby obtaining multiple band gaps with materials having the same lattice parameter, as is the case for III-V alloys. As eluded to previously, forming a GeSn VS can be difficult due to the lack of Sn solubility in Ge and the compressive strain, but both can be compensated by the addition of Si. Si adatoms on a surface are very reactive, as they quickly dissociate water to form SiO_2. The diatomic bond strength for Si-Ge and Si-Sn is greater than Ge-Ge and Sn-Sn, respectively [26]. Therefore, surface Si atoms should readily react with depositing Sn atoms and force Sn incorporation. The atomic size of Si ~4% smaller than Ge and ~20% smaller than Sn; therefore 4

Si atoms should be able to compensate for the larger Sn atoms in the Ge lattice. A SiGeSn layer would not have a direct band gap, but the grading of the Si concentration within the layer should allow for the more gradual strain increase to accommodate thicker GeSn layer growth. A successful GeSn or SiGeSn VS would represent a seminal advance in the development of GeSn for optoelectronics.

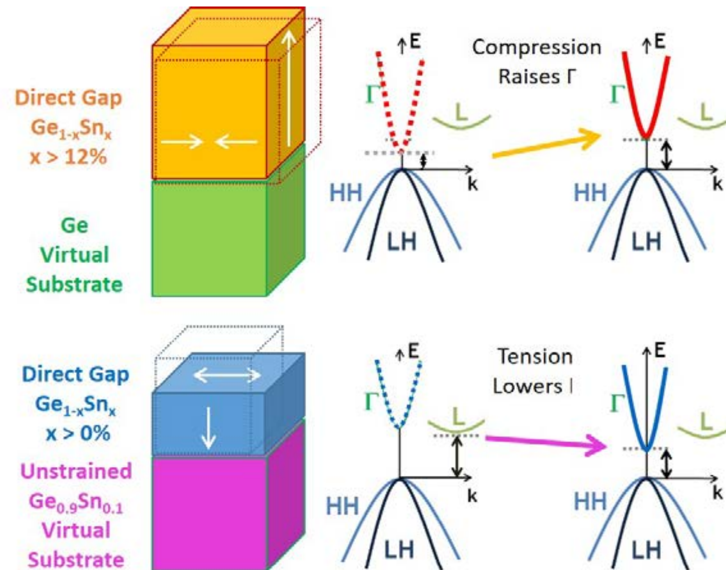

Figure 2. (Top) Compressive strain for GeSn grown on Ge leads to a larger direct band gap requiring greater than 12% Sn to achieve a direct band gap. (Bottom) Growth of GeSn on a $Ge_{0.9}Sn_{0.1}$ VS results in tension for alloys < 10% Sn and a direct band gap. Alloys with Sn > 10 %, while being slightly in compression, will also have a direct band gap.

3. EXPERIMENTS

3.1 Sn and GeSn on Ge VS

Initial efforts were directed at producing, and verifying the utility of, a Ge "virtual substrate" on Si (100) wafers for the growth of GeSn films. The Ge "virtual substrate" is a film of Ge grown on Si at low temperatures and then annealed at much higher temperatures to allow the Ge film to relax. We determined the surface roughness, defect density, and amount of strain relaxation in the Ge virtual substrate. A comparison of the atomic force microscopy (AFM) images of a clean Ge (100) surface to a Ge VS is shown in Figure 3. Although the Ge VS has more morphology than a very flat Ge (100) wafer, the root mean squared (RMS) roughness of both surface is approximately equal. We can see, however, that the cleaned Ge surface can actually suffer from small pits where oxide desorbed during the ultra-high vacuum cleaning process [27]. We found that the Ge virtual substrate was an acceptable replacement for a true Ge (100) substrate and was therefore acceptable for the growth of GeSn films.

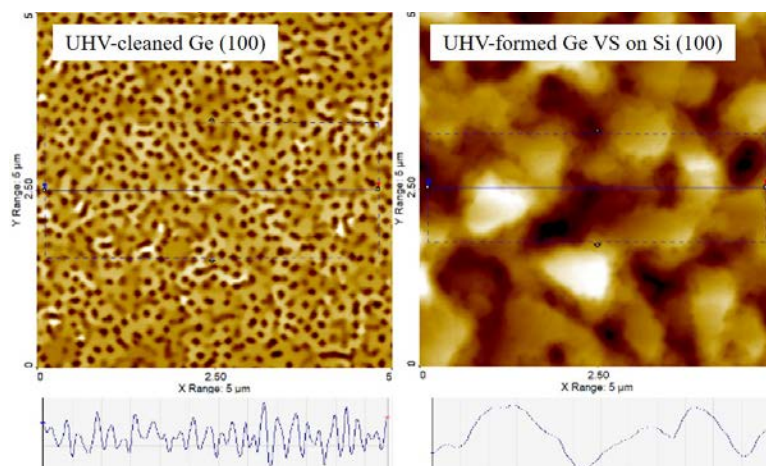

Figure 3. AFM images of (left) Ge (100) surface prepared by a chemical clean and UHV oxide desorption [ref] and (right) a UHV grown Ge VS on Si (100). Below each image is a linescan across the surface.

3.1.1 Sn on Ge and Ge on Sn Studies

Before co-deposition of Ge and Sn to form alloys was undertaken, a study to understand the interaction between the two atoms on the surface was performed. Beginning with a Ge VS, we deposited 200 Å of Sn onto the surface at room temperature. The XPS measurement of the Ge 2p signal from the substrate is shown in Figure 4a. The fact that the Ge signal can be observed indicates two important physical parameters: 1) Sn has a high surface free energy, as it does not cover the Ge surface, and 2) Sn has sufficient adatom mobility from the e-beam evaporation that it can form islands on the surface. The XPS measurement from a 200 Å room temperature deposition of Ge on the 200 Å Sn deposition is shown in Figure 4b. We observe by XPS a complete loss of the Sn signal indicating that Ge has completely covered the Sn surface. This is what one would expect for Ge having a lower surface free energy and sufficient adatom mobility to coat the Sn islands. For the overall growth of a GeSn alloy, if the Sn adatom mobility can be suppressed to prevent islanding, the depositing Ge adatoms can cover the growing surface leading to Sn incorporation.

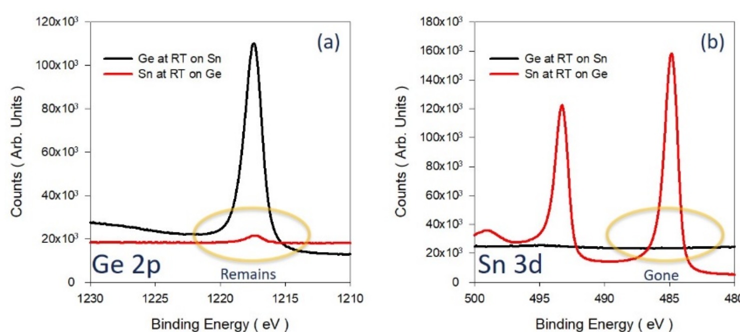

Figure 4. XPS measurements of (a) Ge 2p and (b) Sn 3d after deposition of 200 Å Sn at room temperature on Ge (red curves) and after deposition of 200 Å Ge at room temperature on Sn (black curves).

3.1.2 GeSn on Ge VS

Multiple growth runs have been performed to ascertain the parameters for crystalline $Ge_{0.9}Sn_{0.1}$ films on Ge VS. Literature results indicate that growth should be performed at as low a temperature as possible to minimize Sn segregation and diffusion out from the Ge matrix. We investigated temperatures between room temperature (nominally 25 °C) and 300 °C for a 200 Å $Ge_{0.9}Sn_{0.1}$ alloy that could be the basis for a GeSn VS. XPS measurements of the Ge 2p and Sn 3d signals as a function of growth temperature are shown in Figure 5. Although the Ge and Sn fluxes are nominally identical, which implies identical GeSn composition being deposited, for five growth temperatures, we observed a different surface composition for each temperature. Based on our studies of pure Sn on Ge and Ge on Sn, the spectra for the room temperature deposition is an accurate measure of the depositing flux, as a calculation based on the XPS experimental cross-sections indicates a 10% Sn/90 % Ge composition. For the 50 °C deposition, we see an increase in the Ge 2p signal and a decrease in Sn signal over the room temperature deposition. This phenomenon can best be described by Sn islanding on the surface due to a higher surface adatom mobility for Sn than Ge. For the growths of 100 °C and 150 °C, we see a surface composition that is close to the depositing flux. The deposition at 200 °C has a surface composition that is slightly lower in Ge and higher in Sn than the depositing flux. This is the result of Sn segregation out of the alloy layer due to strain. To avoid Sn segregation, alloy growths should be performed below 200 °C.

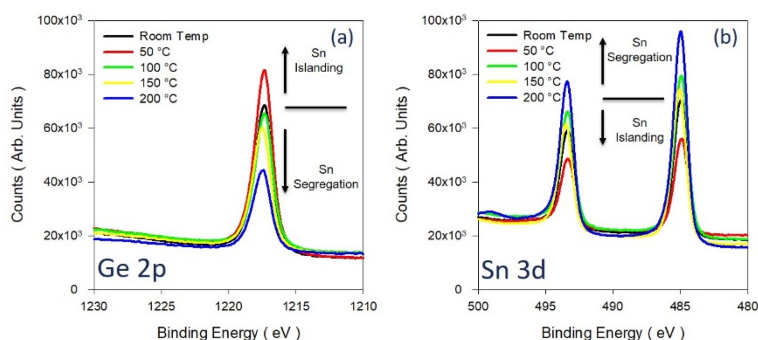

Figure 5: XPS measurement of (a) Ge 2p and (b) Sn 3d as a function of temperature for the growth of a 200 Å $Ge_{0.9}Sn_{0.1}$ alloy on a Ge VS.

In addition to having the correct depositing composition, the alloy formed must also be crystalline. We used low energy electron diffraction (LEED) as an *in vacuo* method for determining surface order and crystallinity in depositing films throughout this research. We found that a growth temperature above 100 °C necessary to obtain a LEED pattern indicative of a crystalline growth. The LEED pattern for GeSn grown on Ge at 200 °C is shown in Figure 6 and is a 2x2 pattern, as seen by the switching of integer order spots by 45° with increasing incident electron energy, and is typical for this alloy deposition. In comparison, also shown in the figure, the Ge VS is a 4x2 pattern. Both patterns are expected for a crystalline orientation on a Si (100) wafer. The diffuse background and broad diffraction spots for the GeSn growth are an indication of poorer surface order and/or surface segregation of Sn on the larger lattice parameter GeSn alloy.

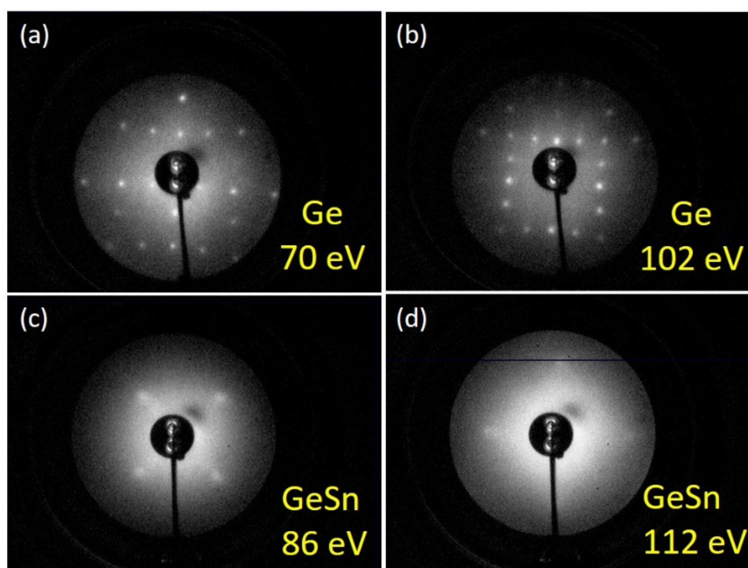

Figure 6. LEED images for Ge VS (a and b) and $Ge_{0.9}Sn_{0.1}$ (c and d) at similar incident energies showing the crystalline nature of GeSn growth.

3.1.3 Sb Surfactant Assisted GeSn Growth on Ge VS

Unique to the MBE growth method is the ability to use a "non-growth" element to act as a surfactant to improve a film's material properties [28], [29]. We found this necessary because the growth of GeSn alloys greater than 200 Å lead to Sn segregation resulting from increased compressive strain as the films grew thicker. We need to grow GeSn alloys thicker than 1000 Å in order to perform x-ray diffraction measurements of strain relaxation and lattice parameter, and we need to grow GeSn alloys greater than 5000 Å in order to perform photoluminescence measurements of band gap and optical properties. By using Sb as a surfactant in the growth of GeSn films, the Sb surface segregation exceeds Sn surface segregation and facilitates the Sn incorporation. By comparing identical growths with and without the use of Sb, we have found that the Sb surfactant does acts to increase the Sn composition in the film, to maintain a smoother growth surface, and to improve the film crystallinity, as measured by x-ray diffraction (XRD) and transmission electron microscopy (TEM). Figure 7 shows the structure, XRD, and TEM results from a 1500 Å $Ge_{0.94}Sn_{0.06}$ alloy grown at 200 °C with a monolayer of Sb atoms used as a surfactant on a Ge VS. The XRD shows the GeSn alloy is under compression, as its out-of-plane lattice constant "$a_{\perp}$" is greater than its in-plane lattice constant "$a_{\parallel}$". The compressive state of the GeSn alloy layer is revealed by the two-dimensional XRD intensity map, which shows that the GeSn peak is situated above that of the Ge VS diffraction spot. Both the GeSn and VS peaks are shifted from the Si substrate due to the relaxation provided by the Ge VS. The sharpness (i.e. narrowness) of a given diffraction peak is a measure of crystalline quality. Given that the Si substrate is a nearly ideal crystal, we find that both the Ge VS and GeSn are highly crystalline (~ 400 arcsec compared to Si at ~40 arcsec) but broadened by the presence of grain boundaries. This departure from perfect crystallinity is confirmed by the TEM image, where misfit dislocations are seen traversing the Ge VS and GeSn layers. The TEM image reveals very abrupt interfaces between layers, which may be attributed to the use of the Sb surfactant. Unfortunately, 6% Sn, incorporated in a Ge film at a growth temperature of 200 °C, does not contain sufficient Sn to produce a direct bandgap, while attempts to grow a 10% Sn alloy with Ge using an Sb surfactant failed due to Sn particle formation.

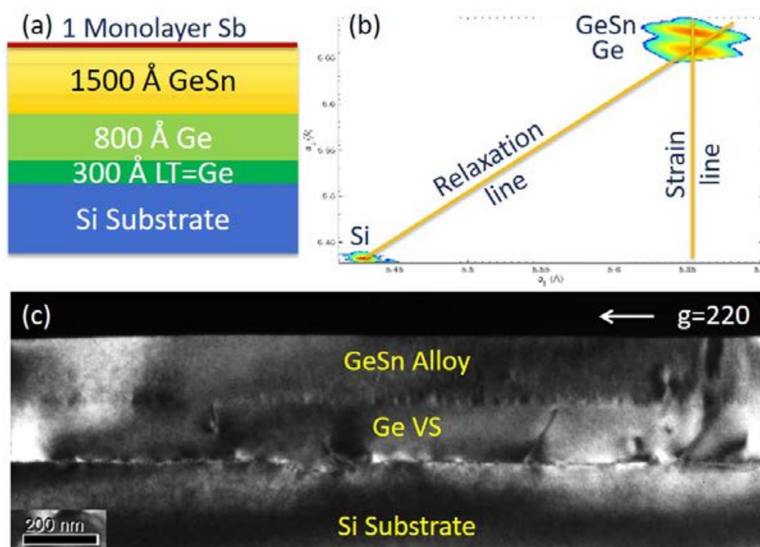

Figure 7. a) Schematic of growth structure; b) XRD results showing relaxed Ge VS and compressively strained GeSn layer; c) TEM results showing abrupt interfaces but having dislocations traversing the Ge VS and the GeSn layers.

3.2 Sn Reactivity on Various Surfaces

3.2.1 Sn on Si, Ge, and Sapphire substrates

Although Sb and Ge have lower surface free energies and can effectively coat a Sn surface, they can not effectively bind (make bonds) to the Sn atoms. This was made apparent during a "growth calibration" run in which the flux would be calibrated against deposition source power (e.g. voltage, current, or temperature) by measuring the mass of the deposited film. In Figure 8, we show the AFM morphology for a Sn calibration growth run deposited on a sapphire wafer (Al_2O_3), a Ge wafer, and a Si wafer at room temperature. In every case the Sn forms islands, but what is relevant in the images is the space between islands. The sapphire surface is terminated with oxygen atoms that are known to effectively bind to Sn. In this case the islands of Sn are numerous and continuous. For the Ge surface, the islands are very large, spaced very far apart, and clearly not bound to the surface. This result was anticipated from the early studies of Sn on Ge and Ge on Sn as measured by XPS in Figure 4. The interesting result is for Sn deposited on the Si surface, where the islands are in-between that for deposition on sapphire or Ge. The Sn deposited on Si shows larger, but fewer, islands than on the sapphire surface, but unlike the Ge surface, the islands are joined along the edges. This indicates that there were fewer nucleation sites that grew outward along the surface before growing vertically, and indicates that there is a favorable interaction between the Sn adatoms and the Si surface.

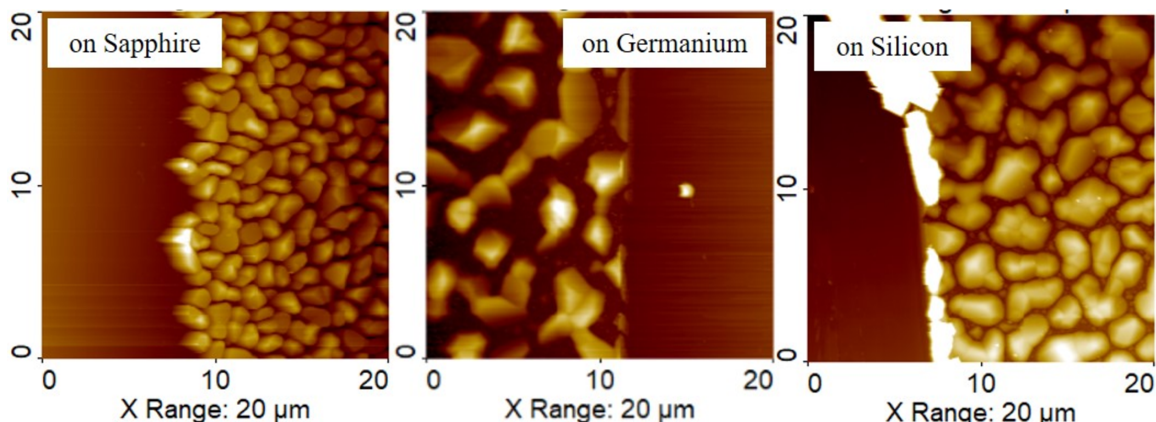

Figure 8. AFM images of MBE growth calibration of 60 minutes of Sn deposited at 7.5 kV and 100 mA on a) sapphire (Al_2O_3), b) Ge, and c) Si wafers to measure mass gain.

3.2.2 Co-depositing Sn and Si on Sapphire

Evaporation of Sn from an e-beam source imparts sufficient energy to the depositing adatoms that they can move on the surface to form islands when the surface has a lower free energy than a Sn surface. This is referred to as a Volmer-Weber (VW) growth mode. There are two other growth modes: Frank van de Merwe (FM) growth is layer by layer growth, where the depositing atoms have a lower surface free energy, and Stranski-Krastanov (SK) growth is layer followed by islanding, where the depositing atoms have lower surface free energy but physical constraints lead to islanding. Growth of Ge on Sn would be an example of FM growth and Ge on Si would be an example of SK growth. Both FM and SK growth modes can lead to epitaxial growth. The formation of Sn islands in VW growth is detrimental to epitaxial growth, and once formed they do not dissolve/merge into the growing film furthering the disruption of growth. Realizing that Sn deposited on a Si surface showed a different interaction than Sn deposited on a Ge surface, we pursued SiSn growth in analogy to GeSn growth. Figure 9 shows the co-deposition of Sn at 0.1 Å/s with differing rates of Si on a sapphire surface where Sn islands should form. We observe that even a small amount of Si ($1/10^{th}$ of the Sn rate) radically changes the surface morphology. No longer do we observe multiple small islands, instead we observe large ridges of material that has accumulated. With increased increase Si rate ($1/5^{th}$ of the Sn rate), we observe only a few islands spaced far apart. Finally, with an equal rate of Si and Sn, there are no islands and the film is smooth and flat. We postulate that by depositing Si with Sn, the Si atom has 4-coordinate bonds that are very reactive, thus bonding quickly to the surface and to other depositing atoms (Sn). Si is also smaller than Sn allowing for some degree of strain compensation. SiSn is an indirect band gap material until it becomes a metal and is not a desired compound, but co-depositing Si with Sn can be used to incorporate Sn in Ge, as Si and Ge are 100% miscible in each other.

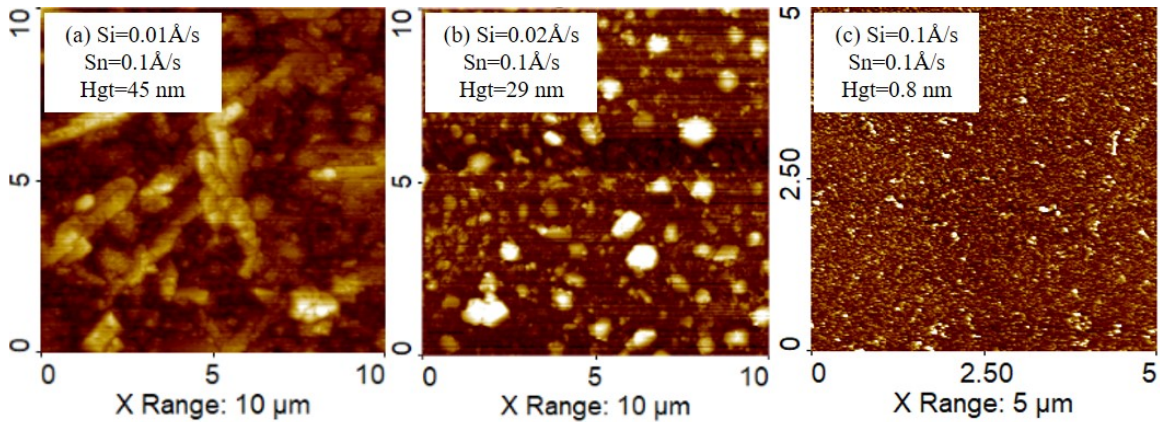

Figure 9. AFM images of co-depositing Sn (at 0.1Å/s) with varying rates of Si a) 0.01Å/s, b) 0.02Å/s, and c) 0.1Å/s on a sapphire surface.

3.3 Developing a SiGeSn VS

3.3.1 SiGeSn on Ge (100) wafer and Ge VS

The thermodynamic growth of GeSn is limited by the solubility of ~1.6% Sn in Ge. Therefore, to get more than 2% Sn into Ge, one must use a kinetically limited growth mode, where the depositing flux more rapidly incorporates than segregates/diffuses out of the forming solid. Our studies show that to accomplish kinetically limited growth, we must control the surface free energy, the depositing adatom mobility, and the reactivity of the growing surface. Utilizing a 0.5 Å/s flux of Ge to effect surface free energy, a ~0.1 Å/s flux of Sn to limit adatom mobility, and a 0.1 Å/s flux of Si to enhance surface reactivity, we were successful at growing a 100 nm 13% Sn alloy for the first time on a Ge (100) surface. To account for strain, the growth was compositionally graded from the Ge wafer to a GeSi alloy before the Sn was introduced and increased to 13%. The XRD measurement for the SiGeSn alloy formed in this manner is shown in Figure 10a. We observe discrete diffraction spots from the individual GeSi layers and from the SiGeSn layers with < 13% Sn oriented vertically from the Ge substrate diffraction spot. This vertical alignment indicates that all of the layers were strained epitaxially to the Ge substrate, with those layers above the Ge being under compression and those layers below being under tension. The final 13% Sn alloy shifts away from vertical alignment due to partial relaxation, and has a lattice parameter of ~5.74 Å, which is equivalent to a 10% Sn alloy without Si. The growth of the $Si_{0.13}Ge_{0.74}Sn_{0.13}$ alloy was accomplished at 135 °C, and thus, this layer composition would be sufficient to act as a VS for the growth of GeSn. However, a thickness greater than 100 nm is needed in order to fully relax the strain.

Beginning with a Ge VS formed on Si, we performed an identical growth program to form a $Si_{0.13}Ge_{0.74}Sn_{0.13}$ to a thickness of 500 nm that was sufficient to result in a nearly complete film relaxation, as determined by XRD shown in Figure 10b. TEM measurements of the SiGeSn film showed that the film was uniform in composition, had no Sn particle inclusion, but was very defective from twinning and misfit dislocations. The high density of dislocations prevents the observation of photoluminescence as a measure of the direct bandgap. However, an infrared transmission measurement was performed to see the absorption band edge of ~0.68 eV (1.8 µm), which is close to the expected value based on the composition derived from a theoretical model. Utilizing the $Si_{0.13}Ge_{0.74}Sn_{0.13}$ alloy as a virtual substrate for the subsequent growth GeSn and SiGeSn alloys has begun with the intention of improving crystal quality to observe direct gap photoluminescence.

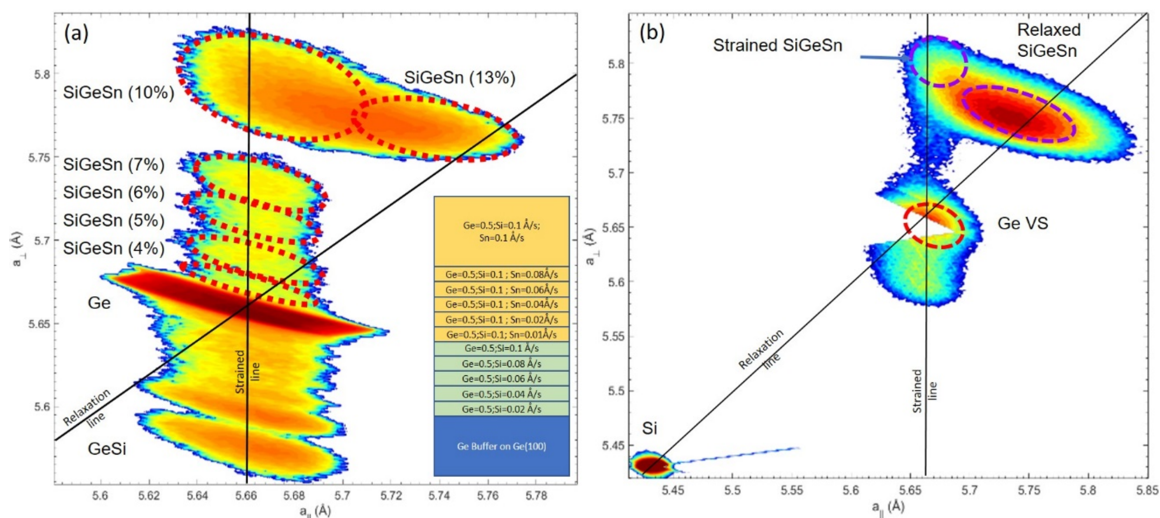

Figure 10. XRD measurements of a $Si_{0.13}Ge_{0.74}Sn_{0.13}$ layer grown on a) Ge (100) wafer, and b) Ge VS formed on Si (100).

3.3.2 SiGeSn on Si (100)

The realization that deposition of Si with GeSn prevented Sn segregation was a major breakthrough and allowed the growth of films with high Sn concentrations (up to 16%). That work was done using a Ge wafer substrate, but the objective of this program is to grow GeSn on a relaxed virtual substrate formed on Si. Through an iterative process, we succeeded in growing a $Si_{0.10}Ge_{0.80}Sn_{0.10}$ relaxed alloy VS on a Si substrate using a step-graded transition from Si to SiGe to GeSi before the SiGeSn alloy. By stepping through the compositions, we were able to observe relaxation begin in the GeSi alloy where the composition was only 70% Ge and 30% Si. All layers after that point were fully relaxed. We successfully created a virtual substrate with a 5.71 Å lattice parameter on a Si substrate for the subsequent growth of GeSn alloys with direct band gaps. The use of a $Si_{0.10}Ge_{0.80}Sn_{0.10}$ VS for the growth of a relaxed, direct gap $Ge_{0.90}Sn_{0.10}$ alloy is shown in Figure 11.

3.4 GeSn on SiGeSn VS

For optical measurements, the GeSn alloys need to be grown thick enough for substantial absorption and emission. We grew an 800-nm-thick 12% Sn alloy on our virtual substrate for testing. An IR absorption measurement shown in Figure 12 has three distinct absorbing layers: GeSn alloy at 3.25 µm, SiGeSn virtual substrate at 2.2 µm, and relaxed GeSi layer at 1.8 µm. The GeSn layer is in the MWIR and has a direct band gap of ~0.4 eV. The SiGeSn virtual substrate is in the SWIR but is an indirect band gap. The GeSi layer is in the NIR at a frequency used by fiber optic telecommunications but is also indirect band gap. Indirect band gap materials are inefficient light emitters, but the direct gap GeSn should be photoexcitable. We attempted to observe photoluminescence from the GeSn, but it was too weak for our experimental setup to detect.

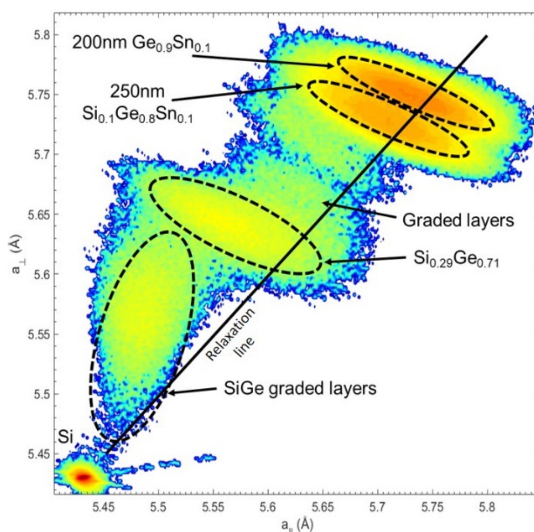

Figure 11. XRD measurement of a 250nm SiGeSn VS formed on Si for the growth of a 200nm GeSn alloy.

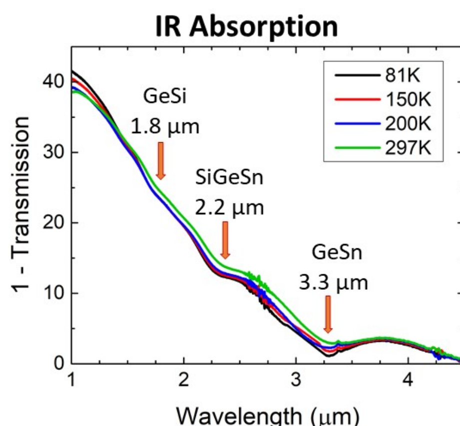

Figure 12: Infrared absorption of $Ge_{0.88}Sn_{0.12}$ alloy grown on a SiGeSn VS formed on a Si (100) surface. We observe an absorbance edge at 3.3 μm, the direct bandgap of the GeSn alloy layer. The absorbance changes at 2.2 μm and 1.8 μm are indirect and are associated with the SiGeSn VS and GeSi transition layer.

XRD, TEM, and energy dispersive x-ray (EDX) analysis shown in Figure 13 of our 800 nm GeSn alloy showed an imperfect material quality, as an explanation for the weak photoluminescence. The XRD results indicate that relaxation begins in the GeSi layer as observed previously, and that all subsequent layers are relaxed. The $Ge_{0.88}Sn_{0.12}$ layer gives rise to intense diffraction due to the layer thickness, although the width of the diffraction peak is due to columnar growth resulting from the use of Si atoms to suppress atom mobility. TEM images also show a a rough interface between the relaxed GeSi layer and the onset of the SiGeSn virtual substrate that may provide nucleation sites for columnar growth. We are currently developing strategies for reducing the roughness of this interface and thereby preventing columnar growth and its associated extended defects. We began a series of experiments growing thicker relaxed buffer layers at a slower rate before the onset of the SiGeSn virtual substrate. This resulted in a less defective, less columnar, and smoother GeSn film with a higher Sn concentration of 16%.

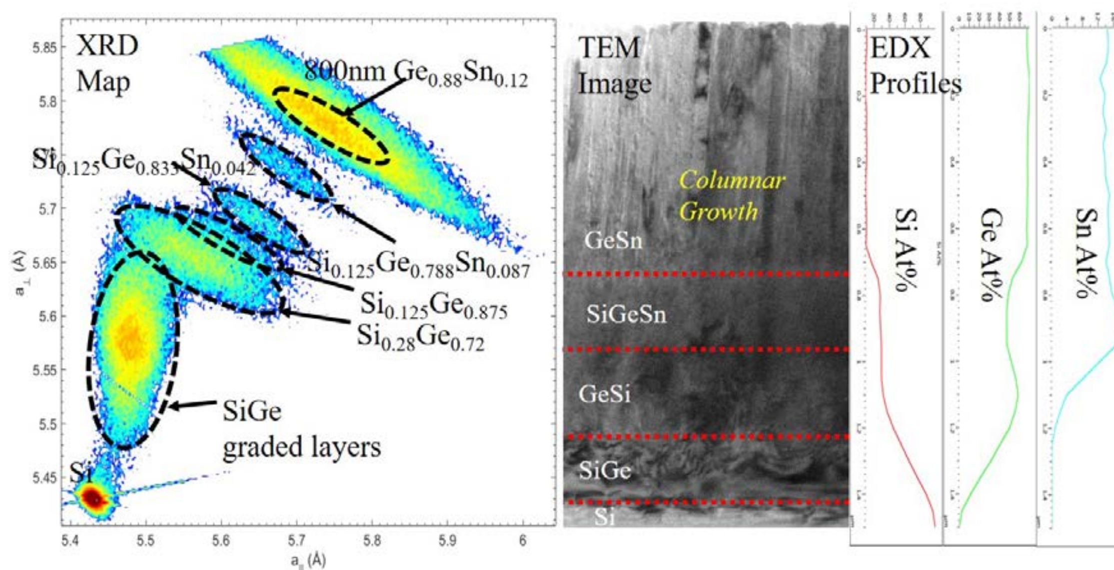

Figure 13: XRD (left), TEM (middle), and EDS (right) of $Ge_{0.88}Sn_{0.12}$ alloy grown on a SiGeSn VS formed on a Si (100) surface.

4. CONCLUSIONS

GeSn is being pursued as a means to directly grow an optoelectronic material on silicon in order to integrate infrared detectors and emitters on Si ROICs without the need for indium bump bonding that limits pixel size and functionality. Successful realization of direct band gap GeSn films grown on a Si substrate was achieved in this program through the use of a SiGeSn virtual substrate. The successful growth had 12% Sn with an IR absorption in the midwave IR at 3.3 µm demonstrating the viability of this approach. Alloys of GeSn can now be grown on the SiGeSn VS to cover the infrared spectrum from communication through to the midwave wavelengths.

The success of the program derives from understanding the chemical interactions between Sn and Ge and between Sn and the substrate. In order to achieve Sn incorporation above the solubility limit, low-temperature, kinetically-limited molecular beam epitaxy was utilized. While Ge has a lower surface free energy and naturally coats a Sn surface, Sn did not form strong bonds with Ge allowing for Sn to segregate and diffuse resulting in Sn particle formation. The use of co-depositing Si, with Ge and Sn, resulted in a more reactive surface that effectively bound the Sn atoms. Thus, a SiGeSn virtual substrate was formed with a sufficiently large lattice parameter that optoelectronic alloys of GeSn could then be subsequently grown without compressive strain. Although the infrared absorption of the GeSn layer was as anticipated, materials improvements are necessary in order to observe infrared emission.

REFERENCES

[1] R. Soref and L. Friedman, "Direct-Gap Ge/Gesn/Si and Gesn/Ge/Si Heterostructures," *Superlattices Microstruct.*, vol. 14, no. 2–3, pp. 189–193, 1993, doi: 10.1006/spmi.1993.1122.

[2] S. Gupta, B. Magyari-Koepe, Y. Nishi, and K. C. Saraswat, "Achieving direct band gap in germanium through integration of Sn alloying and external strain," *J. Appl. Phys.*, vol. 113, no. 7, p. 073707, Feb. 2013, doi: 10.1063/1.4792649.

[3] M. Rojas-Lopez *et al.*, "Raman scattering from fully strained Ge1-xSnx (x <= 0.22) alloys grown on Ge(001)2x1 by low-temperature molecular beam epitaxy," *J. Appl. Phys.*, vol. 84, no. 4, pp. 2219–2223, Aug. 1998.

[4] R. Roucka *et al.*, "Versatile buffer layer architectures based on Ge1-xSnx alloys," *Appl. Phys. Lett.*, vol. 86, no. 19, p. 191912, May 2005, doi: 10.1063/1.1922078.

[5] J. Mathews *et al.*, "Direct-gap photoluminescence with tunable emission wavelength in Ge1−ySny alloys on silicon," *Appl. Phys. Lett.*, vol. 97, no. 22, p. 221912, Nov. 2010, doi: 10.1063/1.3521391.

[6] A. Gassenq *et al.*, "GeSn/Ge heterostructure short-wave infrared photodetectors on silicon," *Opt. Express*, vol. 20, no. 25, pp. 27297–27303, Dec. 2012, doi: 10.1364/OE.20.027297.

[7] J. Mathews, R. Roucka, J. Xie, S.-Q. Yu, J. Menendez, and J. Kouvetakis, "Extended performance GeSn/Si(100) p-i-n photodetectors for full spectral range telecommunication applications," *Appl. Phys. Lett.*, vol. 95, no. 13, p. 133506, Sep. 2009, doi: 10.1063/1.3238327.

[8] H. H. Tseng *et al.*, "Mid-infrared electroluminescence from a Ge/Ge0.922Sn0.078/Ge double heterostructure p-i-n diode on a Si substrate," *Appl. Phys. Lett.*, vol. 102, no. 18, p. 182106, May 2013, doi: 10.1063/1.4804675.

[9] J. Werner *et al.*, "Germanium-tin p-i-n photodetectors integrated on silicon grown by molecular beam epitaxy," *Appl. Phys. Lett.*, vol. 98, no. 6, p. 061108, Feb. 2011, doi: 10.1063/1.3555439.

[10] J. P. Gupta, N. Bhargava, S. Kim, T. Adam, and J. Kolodzey, "Infrared electroluminescence from GeSn heterojunction diodes grown by molecular beam epitaxy," *Appl. Phys. Lett.*, vol. 102, no. 25, p. 251117, Jun. 2013, doi: 10.1063/1.4812747.

[11] M. Oehme *et al.*, "Room-Temperature Electroluminescence From GeSn Light-Emitting Pin Diodes on Si," *Ieee Photonics Technol. Lett.*, vol. 23, no. 23, pp. 1751–1753, Dec. 2011, doi: 10.1109/LPT.2011.2169052.

[12] S. M. Gates, C. M. Greenlief, S. K. Kulkarni, and H. H. Sawin, "Surface reactions in Si chemical vapor deposition from silane," *J. Vac. Sci. Technol. A*, vol. 8, no. 3, pp. 2965–2969, May 1990, doi: 10.1116/1.576614.

[13] L. H. Hall, "The Thermal Decomposition of Germane," *J. Electrochem. Soc.*, vol. 119, no. 11, p. 1593, Nov. 1972, doi: 10.1149/1.2404049.

[14] S. F. A. Kettle, "494. The kinetics of the decomposition of stannane on a tin surface," *J. Chem. Soc. Resumed*, no. 0, pp. 2569–2572, Jan. 1961, doi: 10.1039/JR9610002569.

[15] B. Alharthi *et al.*, "Study of material and optical properties of SixGe1-x-ySny alloys for Si-based optoelectronic device applications," *Opt. Mater. Express*, vol. 7, no. 10, pp. 3517–3528, Oct. 2017, doi: 10.1364/OME.7.003517.

[16] R. Soref, J. Kouvetakis, J. Tolle, J. Menendez, and V. D'Costa, "Advances in SiGeSn technology," *J. Mater. Res.*, vol. 22, no. 12, pp. 3281–3291, Dec. 2007, doi: 10.1557/JMR.2007.0415.

[17] J. Xie, A. V. G. Chizmeshya, J. Tolle, V. R. D'Costa, J. Menendez, and J. Kouvetakis, "Synthesis, Stability Range, and Fundamental Properties of Si-Ge-Sn Semiconductors Grown Directly on Si(100) and Ge(100) Platforms," *Chem. Mater.*, vol. 22, no. 12, pp. 3779–3789, Jun. 2010, doi: 10.1021/cm100915q.

[18] J. S. Harris *et al.*, "MBE Growth of GeSn and SiGeSn Heterojunctions for Photonic Devices," *Sige Ge Relat. Compd. 5 Mater. Process. Devices*, vol. 50, no. 9, pp. 601–605, 2012, doi: 10.1149/05009.0601ecst.

[19] K. R. Khiangte *et al.*, “Dislocation density and strain-relaxation in Ge1−xSnx layers grown on Ge/Si (001) by low-temperature molecular beam epitaxy,” *J. Cryst. Growth*, vol. 470, pp. 135–142, Jul. 2017, doi: 10.1016/j.jcrysgro.2017.04.018.
[20] E. Kasper and M. Oehme, “High speed germanium detectors on Si,” in *Physica Status Solidi C - Current Topics in Solid State Physics, Vol 5,* vol. 5, Y. Hirayama and T. Sogawa, Eds. Weinheim: Wiley-V C H Verlag Gmbh, 2008, pp. 3144–3149.
[21] A. Chroneos, R. W. Grimes, B. P. Uberuaga, S. Brotzmann, and H. Bracht, “Vacancy-arsenic clusters in germanium,” *Appl. Phys. Lett.*, vol. 91, no. 19, p. 192106, Nov. 2007, doi: 10.1063/1.2805773.
[22] J.-H. Choi, K.-D. Na, S.-C. Lee, and C. S. Hwang, “First-principles study on the formation of a vacancy in Ge under biaxial compressive strain,” *Thin Solid Films*, vol. 518, no. 22, pp. 6373–6377, Sep. 2010, doi: 10.1016/j.tsf.2010.03.140.
[23] J. Schulze, M. Oehme, and J. Werner, “Molecular beam epitaxy grown Ge/Si pin layer sequence for photonic devices,” *Thin Solid Films*, vol. 520, no. 8, pp. 3259–3261, Feb. 2012, doi: 10.1016/j.tsf.2011.10.104.
[24] N. Bhargava, M. Coppinger, J. P. Gupta, L. Wielunski, and J. Kolodzey, “Lattice constant and substitutional composition of GeSn alloys grown by molecular beam epitaxy,” *Appl. Phys. Lett.*, vol. 103, no. 4, p. 041908, Jul. 2013, doi: 10.1063/1.4816660.
[25] S. Gupta, “Germanium-Tin (GeSn) Technology,” Ph.D., Stanford University, Dept. of Electrical Engineering, 2013.
[26] “Handbook of Chemistry and Physics 101st Edition.” http://hbcponline.com/faces/contents/ContentsSearch.xhtml (accessed Aug. 06, 2020).
[27] K. Prabhakarana, T. Ogino, R. Hull, J. C. Bean, and L. J. Peticolas, “An efficient method for cleaning Ge(100) surface,” *Surf. Sci.*, vol. 316, no. 1, pp. L1031–L1033, Sep. 1994, doi: 10.1016/0039-6028(94)91117-7.
[28] G. G. Jernigan and P. E. Thompson, “The effect of Sb surfactant assisted growth on SiGe surface morphology,” *Thin Solid Films*, vol. 472, no. 1, pp. 16–19, Jan. 2005, doi: 10.1016/j.tsf.2004.05.117.
[29] G. G. Jernigan, C. L. Silvestre, M. Fatemi, M. E. Twigg, and P. E. Thompson, “Composition and morphology of SiGe alloys grown on Si(100) using an Sb surfactant,” *J. Cryst. Growth*, vol. 213, no. 3, pp. 299–307, Jun. 2000, doi: 10.1016/S0022-0248(00)00369-9.